

PV SYSTEM MODELLING AND SIMULATION USING FLY BASED MICROINVERTER

T. Sindhuja¹, D. Rajababu²

¹PG student [PE&ES], Department of EEE, SR Engineering College, Telangana State, India

²Associate Professor, Department of EEE, SR Engineering College, Telangana State, India

ABSTRACT

This paper proposes simple and efficient modeling approaches that are suitable for long-term and large Photovoltaic (PV) analysis system analyses. Generally it results in slow and inefficient simulations, especially for long-term analyses when transcendental nonlinear equations describing the PV generator, which are coupled with the detailed switching models of the power electronic converters are used. Overcoming this, A classical two-stage power processing system with intermediate dc link used as a string inverter, as well as a single-stage conversion unit using fly back based Micro convertor(MIC) are designed in this paper. This study provides a simplified PV-cell model and its parameterization, Evaluation of maximum power point tracking, Interfacing of photovoltaic (PV) system with Grid. The generalized modeling approach is thoroughly evaluated by the simulation results.

Index Terms—Equivalent circuit, modeling, parameterization, photovoltaic (PV) power system, solar cell.

1. INTRODUCTION

Nowadays the worldwide installed Photovoltaic power capacity shows a nearly exponential increase, despite of their still relatively high cost. This, along with the research for lower cost and higher efficiency devices, motivates the research also in the control of PV inverters, to achieve higher efficiency and reliability. Photovoltaic (PV) power systems are becoming increasingly important with wide acceptance and integration of solar energy in modern electric grids. In recent years, PV power systems have drawn significant research attention, wherein modeling and computer simulation are necessary to analyze the system operation and interaction with utility grids. Over the past decade, various simulation methods have been proposed in the literature works [1]–[9], with significant effort focused on PV modeling and parameterization. However, the proposed parameterization is complex, and the derived PV model requires an iterative solver for simulation implementation. This results in high computational density, which is impractical to simulate large-scale PV power systems using low-cost computer platforms. Besides the study on simulating PV modules and arrays [1]–[9], others focus on either specific PV power systems or certain simulation platforms. For example, in [10], the study focuses on the PV simulation techniques using the RTDS, which is an electromagnetic transients program (EMTP)-based simulation tool. A PV-array model is developed to investigate the side effect of partial shading and module mismatch [11]. One modeling approach is based on the PSIM simulation circuit [12]. In [13], a modeling guideline is developed to simulate three-phase-single-stage PV power systems. Tremendous efforts focus on MATLAB–SIMULINK-based simulation platforms [14]–[17]. These are generally based on specific applications and platforms; therefore, a generalized approach is needed for the efficient modeling and simulation, which is applicable to simulate long-term operation of various PV power systems.

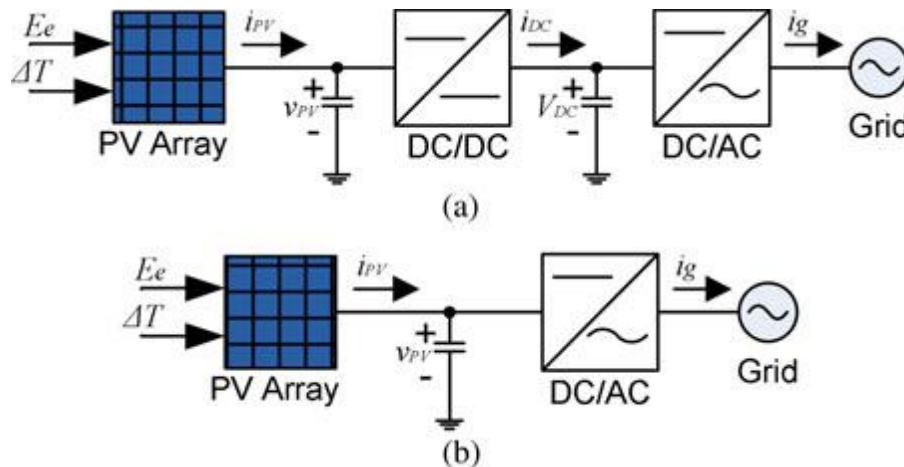


Fig -1: Typical PV power systems. (a) Utility interface is achieved using two converters and IDCL. (b) Utility interface is achieved using single converter without dc link.

Fig. 1 illustrates two typical structures of utility-interactive PV systems, where E_e and ΔT represent the solar irradiance and change in cell temperature, respectively. A system model takes the inputs from the environmental variables, simulates the grid-injection power level, and demonstrates the control and system dynamics. The dc/ac unit can be either single phase or three phase depending on the point of common coupling. Fig. 1(a) shows the two-stage interfacing topology that has an intermediate dc link (IDCL). Because of the high capacitance of the dc link, the dynamic interaction of the dc/dc and dc/ac can be decoupled. Therefore, the control of the dc/dc converter focuses on maximum power injection. The dc/ac inverter performs the dc-link voltage regulation and the grid-tied functions, such as power quality assurance, anti-islanding protection, etc. Fig. 1(b) demonstrates the single-stage interfacing topology that does not have the IDCL. In the single-stage operation, the dc/ac inverter conducts MPPT and other required grid-tied features. The advantage of the single-stage operation lies in the circuit simplicity and higher conversion efficiency than the two-stage solution [18]. However, the dc-link configuration distributes the control into two individual tasks and provides flexibility to implement modular dc/dc MPPT units to achieve better energy harvest [19]. Simulation of such systems requires significant computational power due to the nonlinearity of the PV array and the high-frequency switching of the power interfaces. It is even difficult to simulate hundreds or thousands of inverter based PV systems that are interconnected with a large power network. Following the aforementioned literature review and analysis, a general modeling approach is needed to provide flexibility for any implementation method and efficiency for PV power system simulation. In Section II, a simplified single-diode modeling approach is introduced to parameterize PV-cell models. The model implementation is also provided, including power interface topologies with the IDCL used as string inverters, and single-stage dc/ac conversion, proposed as MICs, which shows advantages in terms of “plug and play” flexibility and solar energy harvest [20].

2. SIMULATION MODELS

Modeling and simulating PV power systems are investigated in this section. By default, all symbols that are used in equations refer to the definition table shown in the Nomenclature.

2.1. Modeling Photovoltaic Cells

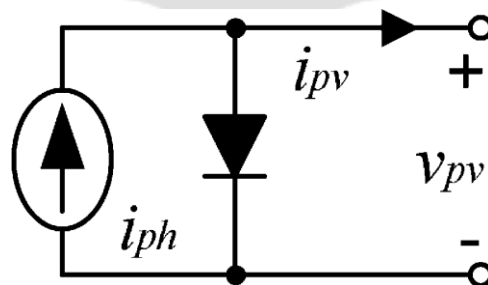


Fig -2: Equivalent circuit for the ideal single-diode PV-cell model.

The ideal single-diode model (ISDM) which is shown in Fig. 2 was proposed to represent PV outputs for crystalline-based solar cells [21], [22]. The simplified model shows computational efficiency but provides fewer

tuning parameters in comparison with the standard single-diode model that was presented in [1]–[3]. The model parameters should be properly identified, and the modeling accuracy should be evaluated carefully before it is integrated into system simulation. The I – V characteristic for an ISDM is expressed as

$$i_{PV} = i_{ph} - i_s \left[e^{\left(\frac{qV_{PV}}{kAT_C} \right)} - 1 \right]. \quad (1)$$

The definition of variables and constants in (1) refers to the nomenclature table. A is an unknown parameter that needs to be identified.

2.2. Photovoltaic Model Parameterization

PV manufacturers provide the values of open-circuit voltage (V_{OCS}), short-circuit current (I_{SCS}), and the maximum power point (V_{MPP} , I_{MPP}) at STC. According to the equivalent circuit of ISDM, the value of the photon current i_{ph} is equal to that of the short-circuit current I_{SCS} at STC. When the solar cell is open-circuited, the output current of a PV cell is zero. Therefore, the I – V characteristics at STC can be expressed as

$$I_{SS} = \frac{I_{SCS}}{e^{\left(\frac{qV_{OCS}}{kAT_{CS}} \right)} - 1} \quad (2)$$

At the MPP of STC, the I – V characteristic equation can be expressed as

$$I_{MPP} = I_{SCS} - I_{SS} \left[e^{\left(\frac{qV_{MPP}}{kAT_{CS}} \right)} - 1 \right] \quad (3)$$

Therefore, the ideality factor A can be derived from (4), shown below, by the substitution of (2) into (3):

$$\frac{e^{\frac{qV_{MPP}}{kAT_{CS}} - 1}}{e^{\frac{qV_{OCS}}{kAT_{CS}} - 1}} = 1 - \frac{I_{MPP}}{I_{SCS}} \quad (4)$$

The diode saturation current I_{SS} can be found by applying A back to (2). Thus, the I – V characteristics at STC can be expressed as (5), shown below, where the photon current and saturation current are constant:

$$i_{PV} = I_{SCS} - I_{SS} \left[e^{\left(\frac{qV_{PV}}{kAT_{CS}} \right)} - 1 \right] \quad (5)$$

2.3. Photovoltaic Model Construction for Simulation

Both the photon current and saturation current change with the solar radiation and cell temperature. For the irradiance deviated from STC, the expression of i_{ph} can be written as

$$i_{ph}(E_e, \Delta T) = \frac{E_e}{E_{STC}} I_{SCS} (1 + \alpha_T \Delta T) \quad (6)$$

where the definitions of E_e and E_{STC} refer to the nomenclature table. ΔT is the temperature difference between the cell temperature T_C and the STC temperature T_{CS} , and α_T is the current temperature coefficient that is given by the product datasheet. The expression in (6) shows that the photon current varies with both solar irradiance and cell temperature. The open-circuit voltage can be derived as

$$V_{OC}(\Delta E_e, \Delta T) = V_{OCS} (1 + \beta_T \Delta T) (1 + \gamma_E \Delta E_e) \quad (7)$$

where the definitions of β_T and γ_E , and E_e and E_{STC} refer to the nomenclature. ΔE_e is the irradiance difference from the STC, and β_T is given by the product datasheet. The irradiance coefficient on voltage γ_E can be determined from the evaluation of the I – V curves for various insolation levels. For example, the open-circuit voltage is given as $V_{OC} 0.8$, when the irradiance is 0.8 kW/m^2 , and the cell temperature is $25 \text{ }^\circ\text{C}$. The value of γ_E can be estimated as

$$\gamma_E = \left(\frac{V_{OC_{0.8}}}{V_{OCS}} - 1 \right) / (1 - 0.8) \quad (8)$$

Therefore, the diode saturation current can be updated by following the environmental variation, which is shown as

$$i_s(\Delta E_e, \Delta T) = \frac{i_{ph}(E_e, \Delta T)}{e^{\left[\frac{qV_{OC}(\Delta E_e, \Delta T)}{kA(T_{CS} + \Delta T)}\right]} - 1} \tag{9}$$

The I-V characteristic equation can be written as (10), shown below, corresponding to the variation of the solar irradiance and cell temperature

$$i_{PV} = i_{ph}(E_e, \Delta T) - i_s(\Delta E_e, \Delta T) \left[e^{\left(\frac{qv_{PV}}{kA(T_{CS} + \Delta T)}\right)} - 1 \right] \tag{10}$$

2.4. Terminal Output Implementation

The single-cell model can be aggregated to any size of a PV array, as shown in Fig. 3.

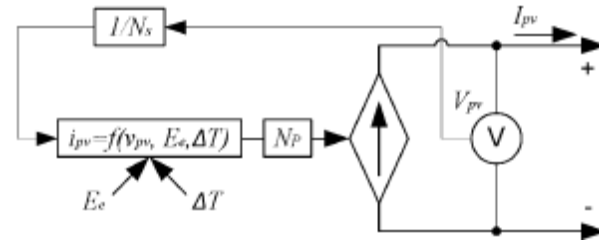


Fig -2: Block diagram of the PV array aggregation and the interconnection interface applicable for commercial simulation software.

Where, N_s and N_p are the numbers of cells that are connected in series and parallel, respectively. When the mathematical representation is combined with a controllable current resource, the model gives terminal outputs regarding to voltage and current V_{pv} and I_{pv} which are compatible with the majority of off-the-shelf circuit-based simulation tools, such as the SimPowerSystems for Simulink, PSIM, PSPICE, PSCAD, etc. The equation, i.e., $i_{pv} = f(v_{pv}, E_e, \Delta T)$, is updated every simulation step following (10) and operating variation. A generalized simulation flowchart is illustrated in Fig. 4.

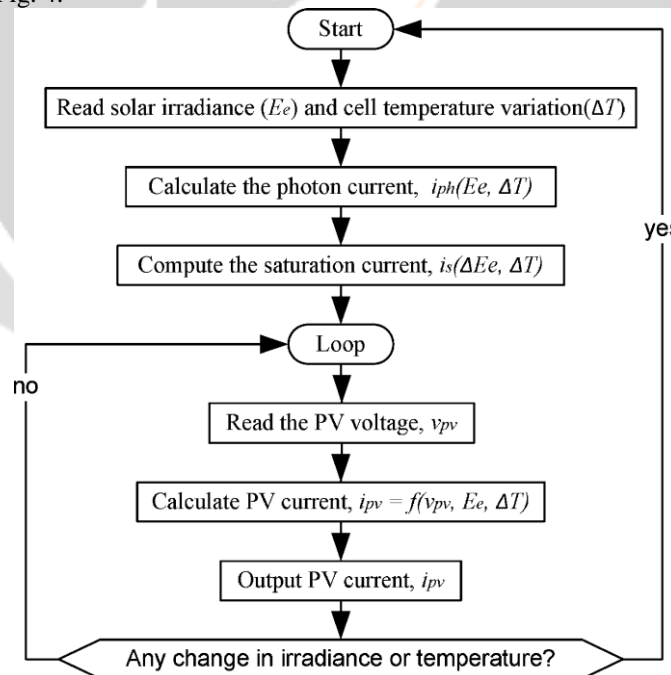


Fig- 4: Flowchart of the PV model simulation.

Unlike the proposed PV model in [1]–[3], the simplified model ignores the coupled terms between i_{pv} and v_{pv} . E_e and ΔT are the environmental variables. The value of v_{pv} is determined by the power equilibrium between the PV generation and load, which is regulated by the interconnected power interface. Therefore, a more efficient simulation can be expected since no iterative solver is needed.

2.5. Interfacing With Intermediate DC Link

For two-stage conversion topologies, as shown in Fig. 1(a), the non isolated dc/dc boost topology is commonly used as the PV front-end power converter (PVFEC) because of the voltage step-up requirement and its simplicity. The control of the PVFEC is the MPPT. One study indicates that the boost topology is superior over the buck in terms of cheaper implementation and better dynamics.

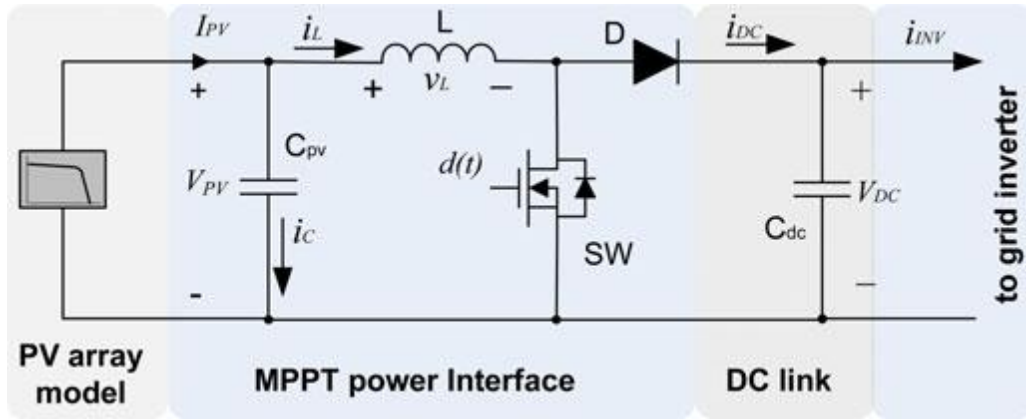


Fig- 5: Circuit schematics showing the combination of the PV array and the dc/dc power interface.

The circuit diagram can be depicted as Fig. 5, where the PV-array model refers to the diagram in Fig. 2, and the IDCL capacitor C_{dc} is the joint connection to dc/ac inverter. Averaged models show advantages of fast simulation if the system switching harmonics are not concerned. This feature is important to simulate a large power system with multiple inverter-based generators. Assuming that the dc/dc converter works in continuous conduction mode (CCM), the averaged model can be derived as

$$\begin{cases} C_{PV} \frac{dV_{PV}}{dt} = I_{PV} - i_L \\ L \frac{di_L}{dt} = V_{PV} - (1-d)V_{dc} \\ C_{dc} \frac{dV_{dc}}{dt} = i_{dc} - i_{INV} \end{cases}$$

$$\Rightarrow \begin{cases} V_{PV} = \frac{1}{C_{PV}} \int (I_{PV} - i_L) dt \\ i_L = \frac{1}{L} \int [V_{PV} - (1-d)V_{dc}] dt \\ V_{dc} = \frac{1}{C_{dc}} \int ((1-d)i_L - i_{INV}) dt \end{cases} \tag{11}$$

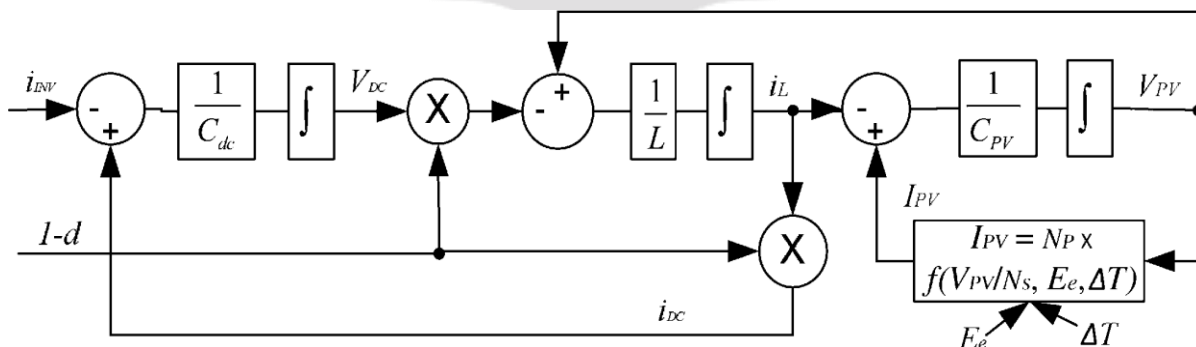


Fig- 6: Implementation of the averaged model in CCM combining the PV array and the boost converter power interface.

Following the expression in (11), the averaged model can be constructed as shown in Fig. 6, where the input variable is the injection current to the grid inverter i_{INV} , the control variable is the duty cycle d , and the state variables include V_{dc} , V_{PV} , and i_L . The environmental inputs that comprise E_e , and ΔT affect the PV-array model output. For the presented two-stage power conversion with IDCL, the values of d and i_{INV} are determined by the MPPT function and V_{dc} regulation, respectively. The output power of dc/ac grid inverters P_{ac} can be estimated as (12), shown below, where the conversion efficiency η can be determined by (13), shown below, applying the peak conversion efficiency η_{max} and the self-power consumption P_{self}

$$P_{ac} = \eta P_{pv} \text{ or } P_{ac} = \eta V_{pv} I_{pv} \tag{12}$$

$$\eta = \frac{(P_{pv} - P_{self}) \times \eta_{max}}{P_{pv}} \tag{13}$$

P_{self} is accumulated power loss that results from microcontrollers, drive circuits, human machine interfaces, other accessories, etc. Since the grid-side voltage is known and steady, the RMS value of the ac injection current can be calculated.

2.6. Interfacing With Grid Without IDCL

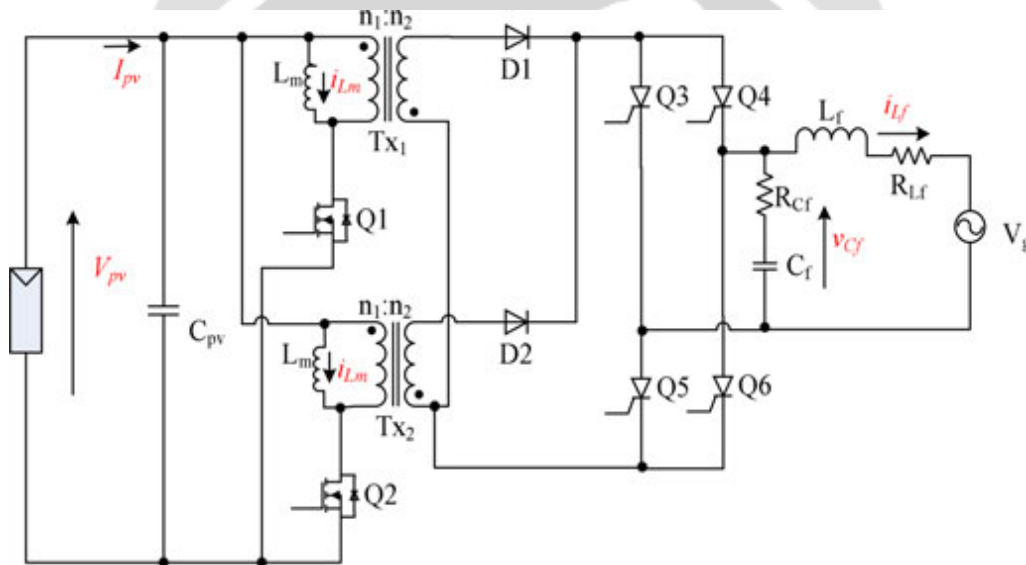


Fig- 7: Topology of the interleaved flyback MIC for solar grid-tied systems.

String inverters show significant generation degradation that results from PV module mismatch and partial shading. The emerging solution is the MIC, which is also called the micro-inverter, to eliminate the power loss that results from inconsistent impacts. A specific MIC, which is shown in Fig. 7 and adopting the interleaved flyback topology, is considered in this study. The topology offers the advantages of high efficiency, reliability, power sharing, galvanic isolation, and reduced PV voltage ripple. Therein, all the details about the converter operation can be found. The simulation model of the MIC is developed by the averaging technique. The model diagram is shown in Fig. 8, where D represents the duty cycle, and $D1$ is defined as $1-D$. The fourth-order dynamic system includes four state variables, v_{pv} , v_{Cf} , i_{Lf} , and i_{Lm} , which result from the input and output storage units and illustrated in the shadowed boxes. In Fig. 8, the boxes with broken lines represent the system inputs, and the duty cycle D is the control variable. The variables V_{pv} and I_{pv} are associated with the PV-panel model.

2.7. Dynamic Model of Maximum Power Point Tracking

The voltage of the optimal operating point (VOOP) is the index that represents the MPP. In this study, it is estimated as

$$V_{OOP}(\Delta E_e, \Delta T) = V_{MPP}(1 + \beta_T \Delta T)(1 + \gamma_E \Delta E_e) \tag{14}$$

where the definitions of β_T and γ_E refer to the nomenclature table. ΔE_e is the irradiance difference from the STC.

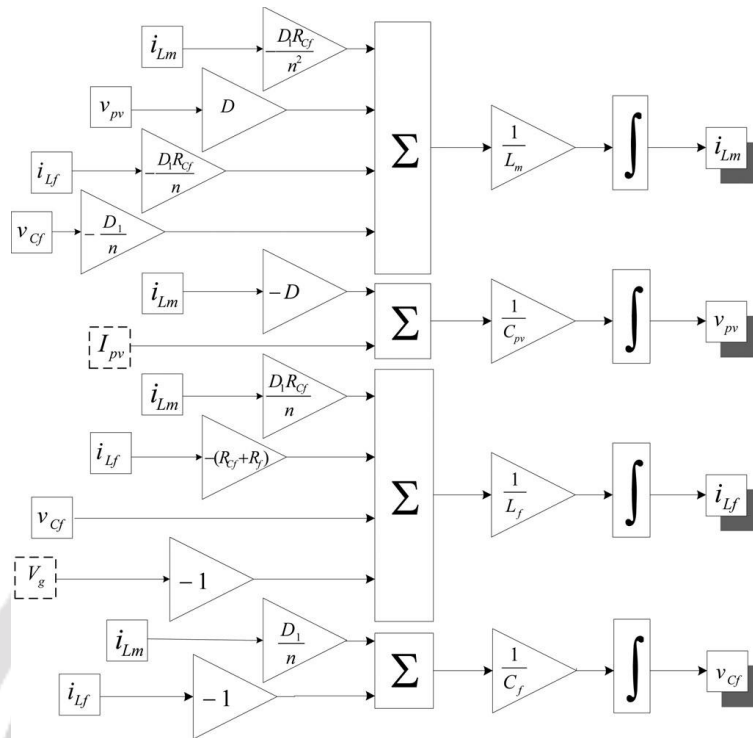


Fig- 8: Averaged simulation model of the flyback-based MIC with current unfolding circuit.

The temperature coefficient can be directly obtained from the product datasheet. The irradiance coefficient on voltage can be determined the evaluation of $I-V$ curves that are based on various insolation levels. One of the commonly used MPPT algorithms is the perturbation and observation (P&O) method [27], which applies two parameters, the perturbation time interval ΔT_{MPPT} and perturbation amplitude ΔV . Thus, the MPP tracking dynamics are implemented by a slew-rate limiter, as expressed in (15), shown below, which defines the maximum rate of the set-point change.

$$SR = \frac{\Delta V}{\Delta T_{MPPT}} \tag{15}$$

As a result, the MPPT operation can be simplified as the diagram shown in Fig. 9, where the optimal operating point is calculated by (14), and the slew-rate limiter mimics the MPP tracking dynamics.

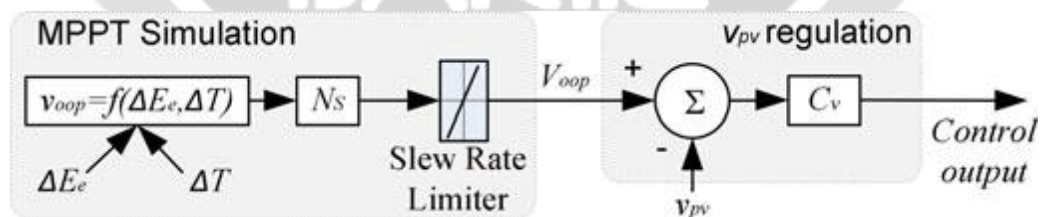


Fig- 9: Proposed simulation implementation of MPPT dynamics using a slew rate limiter.

3. SIMULATION RESULTS AND DISCUSSION

In this section, the evaluation criterion is defined at the beginning. This is followed by simulation evaluation. The simulation platform is the software package of MATLAB/SIMULINK.

3.1. Evaluation Criteria

In this study, the root-mean-square deviation (RMSD) of the current is used to evaluate the modeling accuracy of PV cells. The current RMSD is a measure of the differences between values that are predicted by a model and the values that are actually measured from real systems. For this specific study, the RMSD of the model-generated PV-

current array \tilde{I} with respect to the measured values I is defined as the square root of the mean square error and can be expressed as follows:

$$\text{RMSD}(I) = \sqrt{\frac{\sum_{j=1}^n (\tilde{i}_j - i_j)^2}{n}} \tag{16}$$

$$\tilde{I} = \begin{bmatrix} \tilde{i}_1 \\ \tilde{i}_2 \\ \vdots \\ \tilde{i}_n \end{bmatrix}, \text{ and } I = \begin{bmatrix} i_1 \\ i_2 \\ \vdots \\ i_n \end{bmatrix}$$

Where

The normalized RMSD (NRMSD) of the PV current is the RMSD divided by the range of PV current values which can be expressed as

$$\text{NRMSD} = \frac{\text{RMSD}}{I_{sc}} \tag{17}$$

where I_{sc} is the short-circuit current at STC and represents the upper bound of the PV current. The PV current ranges from zero to the short-circuit current. In this study, the NRMSD is expected to be lower than 3%.

3.2. Photovoltaic Model Evaluation

The evaluation is based on a practical multi-crystalline solar cell which is manufactured by Q-Cells. The model number is Q6LPT3-G2, of which the parameters are given in Table I.

TABLE- I: Data of a Q6LPT3-G2 Multi crystalline Solar cell

Manufacturer:	Q.Cells
Format:	156mm × 156 mm
Open circuit voltage at STC, V_{OCS}	0.613 V
Short circuit current at STC, I_{SCS}	8.34 A
MPP voltage, V_{MPP}	0.511 V
MPP current, I_{MPP}	7.83 A
Temperature coefficient on current, α_T	0.07%/°K
Temperature coefficient on voltage, β_T	-0.36%/°K
Irradiance coefficient on voltage ‡ , γ_E	-0.0528 m ² /kW

[‡]The Irradiance coefficient on voltage, γ_E is estimated by using (8).

Following the parameterization procedure, the ideality factor is derived as $A = 1.43$.

TABLE- II: Modeling Accuracy Following Various Insolation Levels

Test Condition	NRMSD
$E_e = 1.0 \text{ kW/m}^2, T_c = 25^\circ \text{C}$	1.6%
$E_e = 0.8 \text{ kW/m}^2, T_c = 25^\circ \text{C}$	0.7%
$E_e = 0.2 \text{ kW/m}^2, T_c = 25^\circ \text{C}$	2.4%

Table II lists the values of NRMSD following the solar radiation levels. The ISDM shows that the averaged NRMSD is 1.6%, which meets the expectation.

3.3. Evaluation of Maximum Power Point Tracking

In this study, a simplified simulation model is constructed to evaluate the dynamic model of MPPT. The conventional P&O operation is used as the bench mark in comparison with the proposed estimation. The voltage of the optimal operating point VOOP is affected by the solar irradiance changing from 0.2 to 1.0 kW/m². In a typical grid-tied PV system, the array voltage is usually rated from 200 to 1000 V. therefore, the VOOP estimation is based on the configuration that 1080 Q6LPT3-G2 solar cells are in series connection. The simulation shows that both the

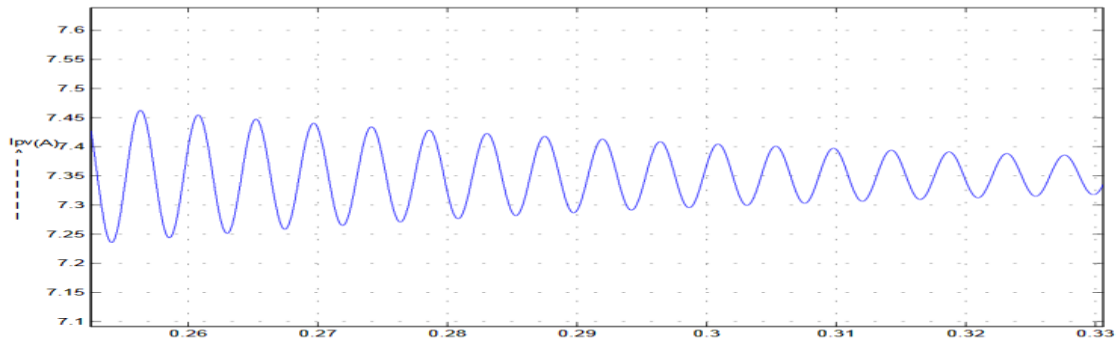
P&O algorithm and the proposed estimation can follow the thermal change and indicate the variation of optimal operating points.

3.4. Interfacing With Grid Without IDCL

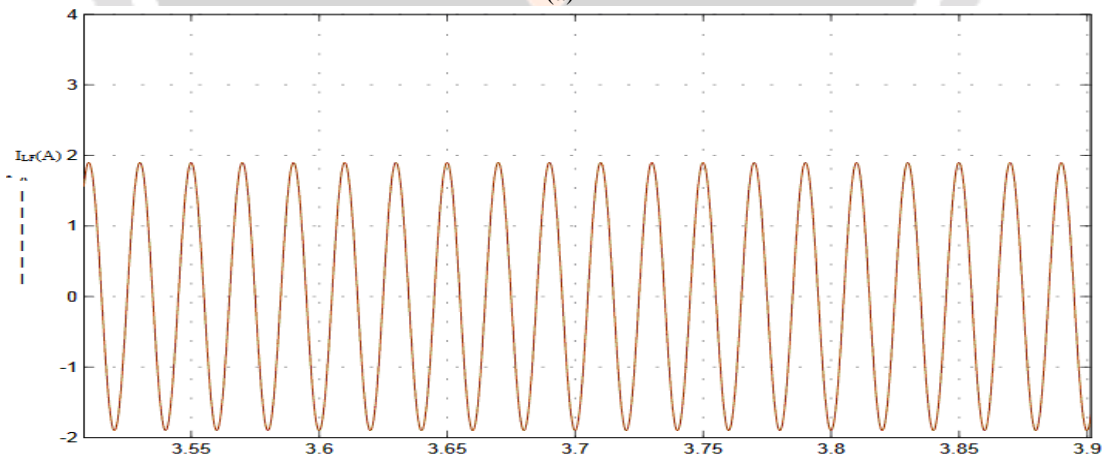
The MIC model is rated as 300W for the simulation purpose. It is connected to a solar panel, which is constructed by 72 Q6LPT3-G2 cells in series connection. Thus, the peak power of the PV module is rated as 288.2 W, and the optimum terminal voltage is 36.81 V to represent the MPP. The system parameters are listed in Table III, of which the symbols refer to the diagram shown in Figs. 7 and 8.

Table- III: Interleaved fly back MIC circuit parameters

PV capacitor	C_{pv}	18 mF
Inductance	L_m	28 μ H
Transformer turns ratio	n_2/n_1	12
Capacitor ESR	R_{Cf}	1 m Ω
Filter capacitor	C_f	0.092 μ F
Filter inductor	L_f	300 μ H
Inductor ESR	R_f	0.24 Ω
Grid side voltage	V_g	342V _{pk} , 50Hz
Switching frequency	f_{sw}	172 kHz



(a)



(b)

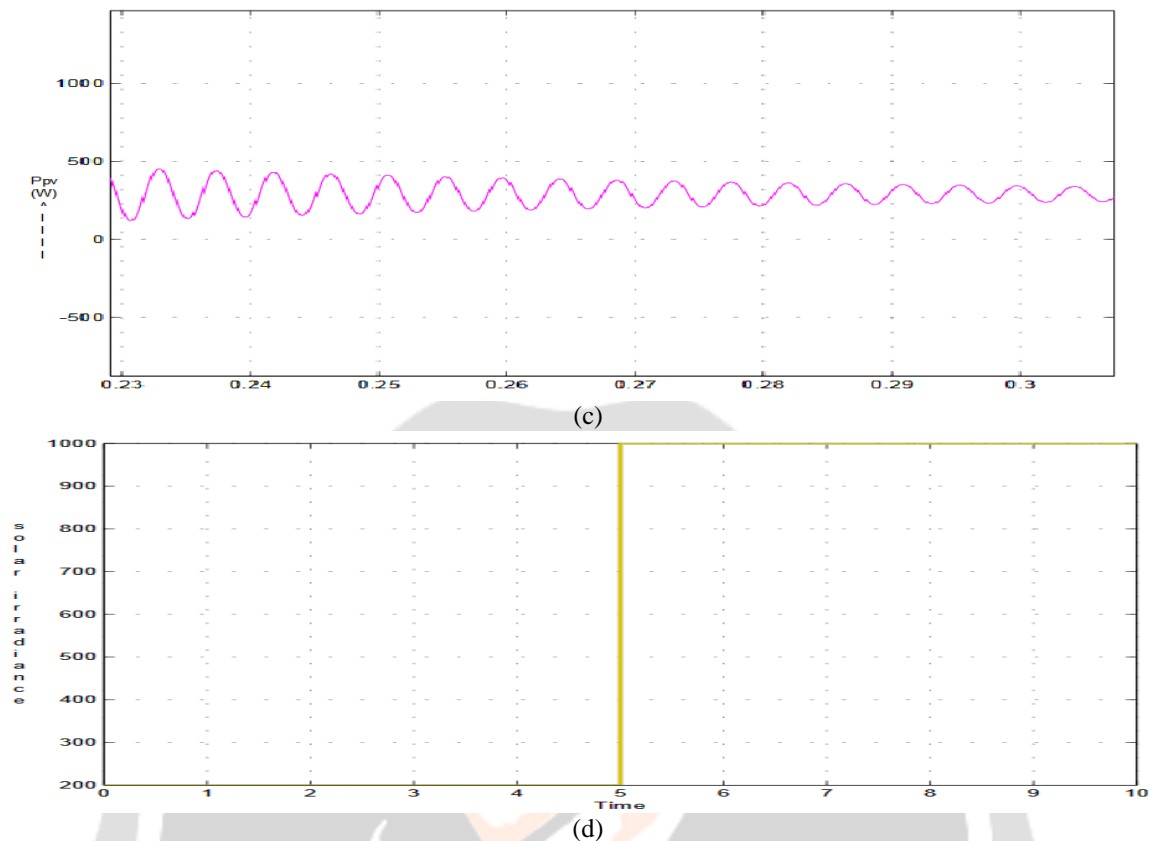


Fig-12: Simulated waveforms generated by the proposed MIC model (a) PV current, (b) ac output current (c) PV power and (d) Solar Irradiance.

Fig. 12 illustrates the reference signal in comparison with the waveforms that are generated by the proposed average model, which is formulated to simulate the detailed switching operation using Simulink and Sim Power-Systems. It covers all the details of switching operation including the sine-triangle modulation. Due to the high-switching frequency, i.e., 172 kHz, the simulation configuration applies a variable step engine with the maximum step size of 1×10^{-7} s. The simulation platform is a personal computer (PC) with one Intel i7-2600 CPU and 16-GB RAM. It takes 1.5102×10^5 s, which is approximately 42 h, to simulate a 100-ms operation of the MIC grid-tied system. This implies that the integration of the physical modeling approach and single-PC platform is impossible to simulate a large power system imagining that hundreds or thousands MICs are interconnected with the grid. Under the same simulation condition, the proposed averaged model uses 47.45 s to fulfill the 100-ms operation including the maximum power tracking, dc/ac conversion, and power quality control. The proposed approach demonstrates the simulation speed advantage in comparison with the conventional physical model. Fig. 12 illustrates the waveforms of PV current i_{pv} , ac current i_{Lf} , and PV power P_{pv} , which are simulated by the presented MIC model.

4. CONCLUSION

This paper has presented a general approach to modeling and simulating PV power systems with regard to electrical engineering perspectives. A simplified PV model is developed showing the detailed parameterization, which is based on the given information of the datasheet. Since the majority of PV power system is grid-tied, the modeling process focuses on two common power interfaces that include the two stage power conversion with IDCL and single-stage conversion without IDCL. The MIC that is called “micro-inverter” is also included for the simulation study. Due to the high-frequency switching nature of the MIC, the proposed averaged modeling approach demonstrates a simulation speed advantage, which is significantly faster than the conventional physical model. The simplified PV model is thoroughly evaluated by the MATLAB/SIMULINK.

REFERENCES

- [1] M. G. Villalva, J. R. Gazoli, and E. R. Filho, "Comprehensive approach to modeling and simulation of photovoltaic arrays," *IEEE Trans. Power Electron.*, vol. 24, no. 5, pp. 1198–1208, May 2009.
- [2] F. Caracciolo, E. Dallago, D. G. Finarelli, A. Liberale, and P. Merhej, "Single-variable optimization method for evaluating solar cell and solar module parameters," *IEEE J. Photovoltaics*, vol. 2, no. 2, pp. 173–180, Apr. 2012.
- [3] A. Ortiz-Conde, D. G. Lugo-Muñoz, and F. J. García-Sánchez, "An explicit multiexponential model as an alternative to traditional solar cell models with series and shunt resistances," *IEEE J. Photovoltaics*, vol. 2, no. 3, pp. 261–268, Jul. 2012.
- [4] D. Sera, R. Teodorescu, and P. Rodriguez, "PV panel model based on datasheet values," in *Proc. IEEE Int. Symp. Ind. Electron.*, 2007, pp. 2392–2396.
- [5] A. N. Celik and N. Acikgoz, "Modelling and experimental verification of the operating current of mono-crystalline photovoltaic modules using four- and five-parameter models," *Appl. Energy*, vol. 84, pp. 1–15, 2007.
- [6] W. D. Soto, S. A. Klein, and W. A. Beckman, "Improvement and validation of a model for photovoltaic array performance," *Sol. Energy*, vol. 80, pp. 78–88, 2006.
- [7] S. Liu and R. A. Dougal, "Dynamic multiphysics model for solar array," *IEEE Trans. Energy Convers.*, vol. 17, no. 2, pp. 285–294, Jun. 2002.
- [8] J. A. Gow and C. D. Manning, "Development of a photovoltaic array model for use in power-electronics simulation studies," *IEE Proc. Electr. Power Appl.*, vol. 146, no. 2, pp. 193–200, Mar. 1999.
- [9] M. A. Hamdy and R. L. Call, "The effect of the diode ideality factor on the experimental determination of series resistance of solar cells," *Sol. Cells*, vol. 20, pp. 119–126, 1987.
- [10] P. Minwon and Y. In-Keun, "A novel real-time simulation technique of photovoltaic generation systems using RTDS," *IEEE Trans. Energy Convers.*, vol. 19, no. 1, pp. 164–169, Mar. 2004.
- [11] N. D. Kaushika and N. K. Gautam, "Energy yield simulations of interconnected solar PV arrays," *IEEE Trans. Energy Convers.*, vol. 18, no. 1, pp. 127–134, Mar. 2003.
- [12] M. Veerachary, "PSIM circuit-oriented simulator model for the nonlinear photovoltaic sources," *IEEE Trans. Aerosp. Electron. Syst.*, vol. 42, no. 2, pp. 735–740, Apr. 2006.
- [13] A. Yazdani, A. R. Di Fazio, H. Ghoddami, M. Russo, M. Kazerani, J. Jatskevich, K. Strunz, S. Leva, and J. A. Martinez, "Modeling guidelines and a benchmark for power system simulation studies of three-phase single-stage photovoltaic systems," *IEEE Trans. Power Del.*, vol. 26, no. 2, pp. 1247–1264, Apr. 2011.
- [14] R. Rahmani, M. Fard, A. A. Shojaei, M. F. Othman, and R. Yusof, "A complete model of stand-alone photovoltaic array in matlab-simulink environment," in *Proc. IEEE Student Conf. Res. Develop.*, 2011, pp. 46–51.
- [15] N. Pandiarajan and R. Muthu, "Mathematical modeling of photovoltaic module with simulink," in *Proc. 1st Int. Conf. Electr. Energy Syst.*, 2011, pp. 258–263.
- [16] J. R. Rodriguez, F. Ruiz, D. Biel, and F. Guinjoan, "Simulation and analysis of distributed PV generation in a LV network using MATLABSimulink," in *Proc. IEEE Int. Symp. Circuits Syst.*, 2010, pp. 2322–2325.
- [17] G. Walker, "Evaluating MPPT converter topologies using a MATLAB PV model," *J. Elect. Electron. Eng., Aust.*, vol. 21, pp. 45–55, 2001. 508 IEEE JOURNAL OF PHOTOVOLTAICS, VOL. 3, NO. 1, JANUARY 2013.